

Submarine Automatic Control

Dr Peter Ridley

School of Mechanical Engineering,
Queensland University of Technology,
GPO Box 2434, Brisbane 4001, Australia,
p.ridley@qut.edu.au

Julien Fontan and Dr Peter Corke

CSIRO Manufacturing Science and Technology,
QCAT PO Box 883, Kenmore 4069,
Australia,
peter.corke@csiro.au

Abstract

This paper investigates the automatic attitude and depth control of a torpedo shaped submarine. Both experimental results and dynamic simulations are used to tune feedback control loops in order to obtain stable control of yaw, pitch and roll of the craft.

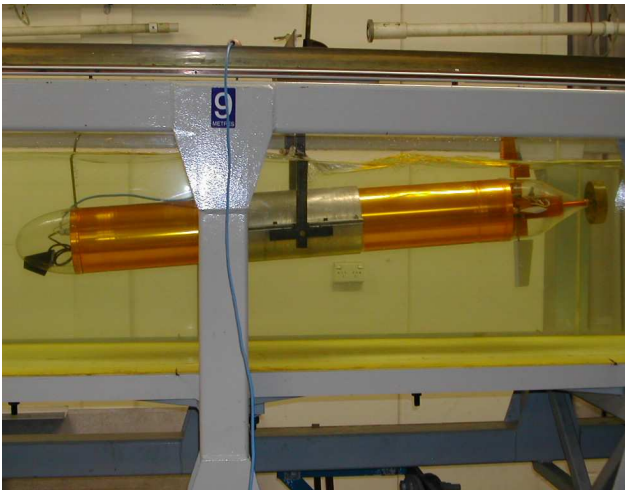


Figure 1: Full size submarine pivoted in the flume

Introduction

This paper takes a non-linear multi degree of freedom mathematical model from [Ridley, Fontan, Corke 2003] and applies it to the implementation of automatic control loops which regulate the attitude (pitch, roll and yaw) of the submarine shown in Figure 1. On the basis of first principles calculations of force/moment coefficients, this non-linear model is reduced to a set of uncoupled, transfer functions which describe the yaw, pitch and roll dynamics of the submarine. Experimental data obtained from the full-size submarine, horizontally pivoted, in a flume is used to validate the pitch

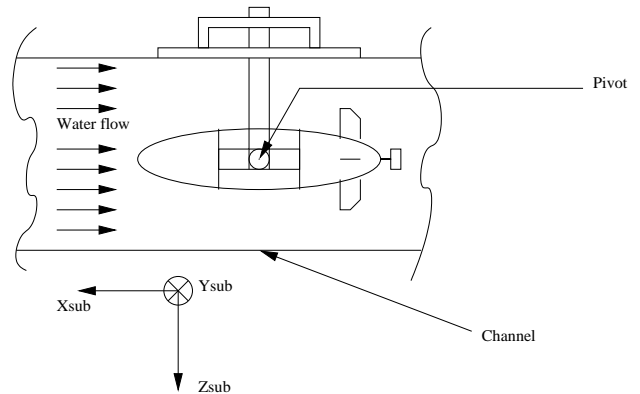


Figure 2: Experimental setup

transfer function and to determine suitable controller gains to tune the pitch control loop. A depth control loop is also constructed and its controller gains tuned by simulation. Feedback control of yaw and roll axes is investigated, and appropriate controller gains are estimated using simulation.

Experimental setup

Figure 2 shows the experimental setup used to analyse the dynamic open and closed loop behavior of the submarine. The submarine is immersed in a flume 585mm wide through which water flows at rates up to 200 litres/sec. Water depth, which determines the water speed (V) is controlled by a weir at the end of the flume. In this setup the submarine is restrained in a cradle, which allows it to pivot about a horizontal axis through its centre of gravity.

Linearised Transfer Functions

The following non-linear differential equations, calculated in a body centred coordinate frame, describe change of attitude of a submarine (mass m , inertia $[I_{xx}, I_{yy}, I_{zz}]$) whose velocity is $\mathbf{V} = [u, v, w]^T$.

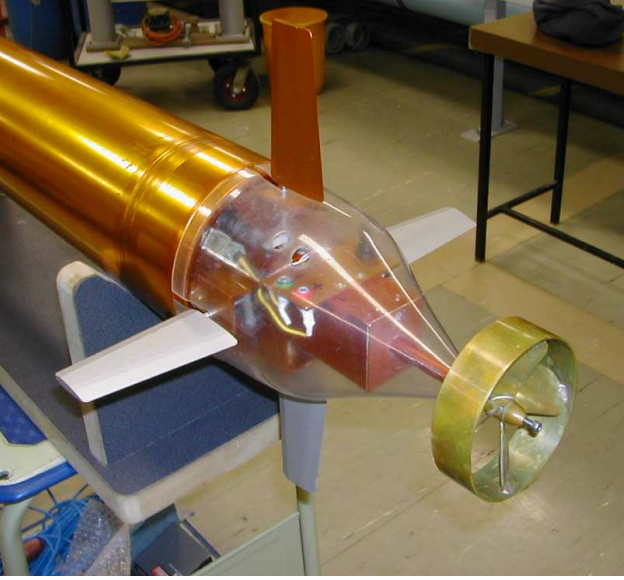


Figure 3: Submarine control surfaces.

$$I_{xx}\dot{p} + (I_{zz} - I_{yy})qr - m[y_G(\dot{w} - uq + vp) - z_G(\dot{v} - wp + ur)] = \sum K_{ext}$$

$$I_{yy}\dot{q} + (I_{xx} - I_{zz})rp - m[z_G(\dot{u} - vr + wq) - x_G(\dot{w} - uq + vp)] = \sum M_{ext}$$

$$I_{zz}\dot{r} + (I_{yy} - I_{xx})pq - m[x_G(\dot{v} - wp + ur) - y_G(\dot{u} - vr + wq)] = \sum N_{ext} \quad (1)$$

Nett external moments ($\sum K_{ext}, \sum M_{ext}, \sum N_{ext}$) acting on the submarine are:

$$\begin{aligned} \sum K_{ext} &= K_{HS} + K_p\dot{p} + K_{uu}\delta_r (-\delta_{r_{top}} + \delta_{r_{bottom}}) + \\ &\quad K_{uu}\delta_s (-\delta_{s_{right}} + \delta_{s_{left}}) + K_{prop} \\ \sum M_{ext} &= M_{HS} + M_{uu}\delta_s u^2\delta_s + M_{uw}uw + M_{uq}uq + \\ &\quad M_{vp}vp + M_{\dot{w}}\dot{w} + M_{\dot{q}}\dot{q} + M_{rp}rp \\ \sum N_{ext} &= N_{HS} + N_{uu}\delta_r u^2\delta_r + N_{ur}ur + N_{uv}uv + \\ &\quad N_{\dot{v}}\dot{v} + N_{wp}wp + N_{pq}pq + N_{\dot{r}}\dot{r} \end{aligned} \quad (2)$$

and the resulting angular velocity is $\omega = [p, q, r]^T$.

Assuming that changes of attitude, measured in Euler angles for roll, pitch and yaw (ϕ, θ, ψ), are small, the hydrostatic moments acting on the submarine, about its centre of buoyancy, are:

$$\begin{aligned} K_{HS} &= -y_G W - z_G W \phi \\ M_{HS} &= -z_G W \theta - x_G W \\ N_{HS} &= -y_G W \phi - z_G W \theta \end{aligned} \quad (3)$$

If these small angle approximations are substituted into the combined equations 1 and 2, writing $\dot{\phi} = p, \dot{\theta} = q, \dot{\psi} = r$ and ignoring negligibly small quantities, the linearised transfer functions for yaw, pitch and roll are :

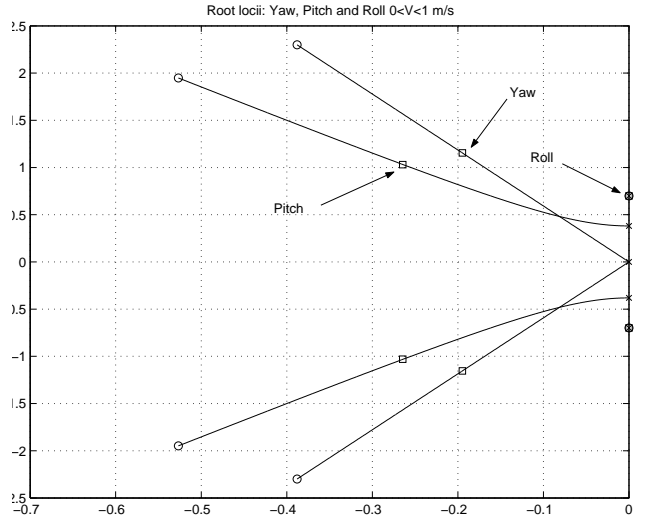


Figure 4: Root locus: Yaw, pitch and roll poles vs submarine speed. Squares indicate pole positions for $V=0.5$ m/s.

$$\frac{\psi(s)}{\delta_r(s)} = \frac{\left(\frac{2N_{uu}\delta_r}{N_{uv}}\right)}{\left(\frac{I_{zz}-N_{\dot{r}}}{N_{uv}V^2}\right)s^2 + \left(\frac{-mX_g-N_{ur}}{N_{uv}V^2}\right)Vs + 1} \quad (4)$$

$$\frac{\theta(s)}{\delta_s(s)} = \frac{\left(\frac{2M_{uu}\delta_s V^2}{Z_g W - M_{uw} V^2}\right)}{\left(\frac{I_{yy}-M_{\dot{q}}}{Z_g W - M_{uw} V^2}\right)s^2 + \left(\frac{mX_g - M_{uq}}{Z_g W - M_{uw} V^2}\right)Vs + 1} \quad (5)$$

$$\frac{\phi(s)}{\delta_a(s)} = \frac{\left(\frac{4K_{uu}\delta_a}{Z_g W}\right)}{\left(\frac{I_{xx}-K_p}{Z_g W}\right)s^2 + 1} \quad (6)$$

where:

- $(\delta_r, \delta_s, \delta_a)$ are the rudder, stern plane, aileron angles,
- $N_{uu\delta_r}, M_{uu\delta_s}, K_{uu\delta_a}$ rudder, stern plane, aileron effectiveness,
- N_{ur}, M_{uw} (body moment),
- $N_{\dot{r}}, M_{\dot{q}}, K_p$ (added mass),
- N_{ur}, M_{uq} (added mass cross term) are hydrodynamic coefficients,
- X_g, Z_g are the coordinates of the CG relative to the centre of buoyancy.

Numerical estimates of these are tabulated in the Appendix of this paper.

These transfer functions are quadratic lags of the form:

$$\frac{\theta(s)}{\delta_s(s)} = \frac{K}{\frac{s^2}{\omega_n^2} + \frac{2\xi}{\omega_n}s + 1}, \quad (7)$$

Figure 4 shows the root locii of the poles of these transfer functions as the submarine speed V increases.

Dynamics for yaw and pitch both depend on speed whereas the roll dynamics are insensitive to speed. Roll dynamics exhibit marginally stable poles. Open loop yaw response and pitch responses are both oscillatory but stable.

DC gain K of the yaw and roll transfer functions are invariant with speed, whereas the DC gain of the pitch transfer function varies with speed as shown in Figure 5.

Natural frequency and damping ratio of the pitch poles is plotted in Figure 6. Both yaw and pitch responses exhibit natural frequencies which are essentially directly proportional to the waterspeed.

Positioning of the centre of gravity below the centre of buoyancy (Z_g positive) gives the pitch response a little more damping than the yaw response. It also causes the damping ratio of the pitch response to increase asymptotically toward a constant value (Figure 7) whereas the damping ratio of the yaw response is invariant with speed.

Damping ratio of the yaw and pitch modes is very sensitive to the estimate of X_g , the position of the centre of gravity relative to the centre of buoyancy.

Experimentally measured open-loop, pitch angle responses to a stern plane, step input (Figure 8) exhibit overshoot and transient decay to a steady state, which are characteristic of a second order, underdamped response identified in equations 5 and 7. When numerical values are substituted for the parameters contained in equation 5, a theoretical estimate of the natural frequency of 1.1 rad./sec. obtained. This figure is smaller than the experimentally measured value of 2.8 rad/sec, observed in Figure 8.

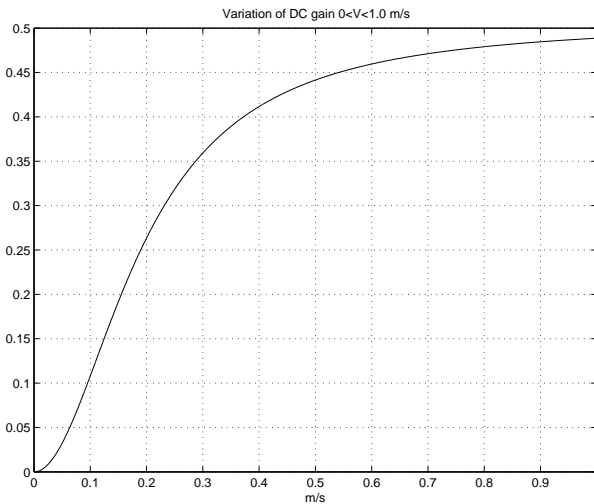


Figure 5: Open loop pitch response: DC Gain K vs submarine speed

Pitch angle control

Incorporating an inclinometer into a feedback loop and tuning the loop with a PID controller allows us to ob-

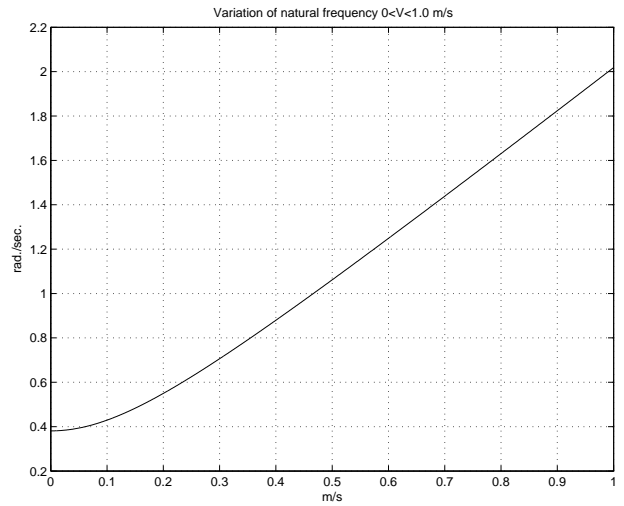


Figure 6: Open loop pitch response: Natural frequency ω_n vs submarine speed

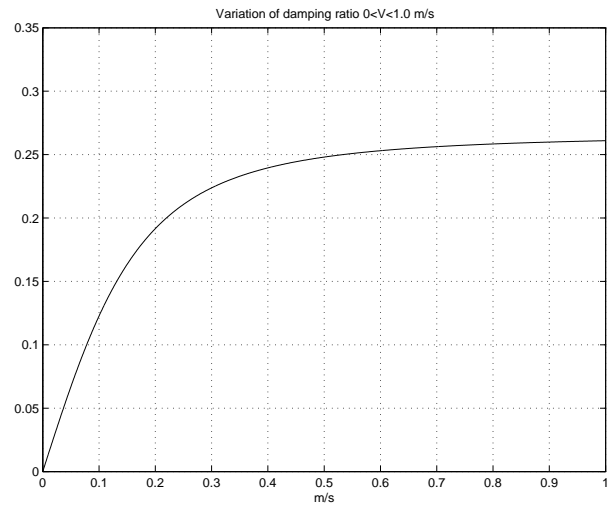


Figure 7: Open loop pitch response: Damping ratio ξ vs submarine speed

tain automatic control of pitch angle. Initially the control loop was tuned with proportional gain alone. The pitch angle response of the submarine to step inputs of the command input to the loop are shown at two different water speeds in Figures 9 and 10. As the speed increases, the response shows a marked reduction in steady state error and a less damped transient response. These changes are a direct effect of the increasing DC gain of the transfer function noted in Figure 5.

Integral and derivative gains were added to improve the steady state error characteristic exhibited when proportional control alone is used. The root locus diagram, shown in Figure 11, shows that the system is unconditionally stable. Three active poles dictate the loop dynamics. A dominant first order pole, close to the origin, causes a slow drift which removes the

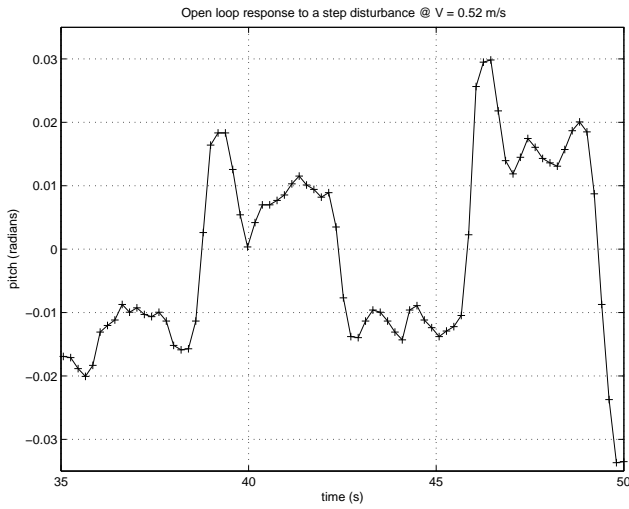


Figure 8: Open loop pitch disturbance response: $\omega_n=2.8$ r/sec. and $\xi = 0.25$

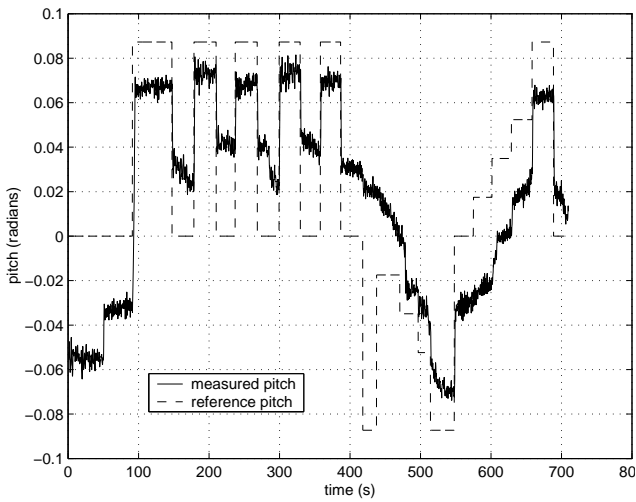


Figure 9: Closed loop pitch command response: $V=0.618$ m/sec. $k_p=11$

steady state error. The pair of quadratic poles provide an oscillatory component of response superimposed on top of this drift. Theoretical pitch command step response, based on a linear model, is shown in Figure 12 and can be compared with the experimentally measured responses plotted in Figure 13. Figure 13 shows that in the actual response, steady state error is more quickly eliminated than is theoretically predicted. This is possibly due to the unmodelled non-linearities in the actual system.

The controller has a saturation limit imposed which prevents the fin exceeding its stall angle of 14° . Saturation dictates the upper useful limit to which the proportional gain can be increased. Measured response of the submarine pitch angle to impulse disturbance inputs is shown in Figure 14.

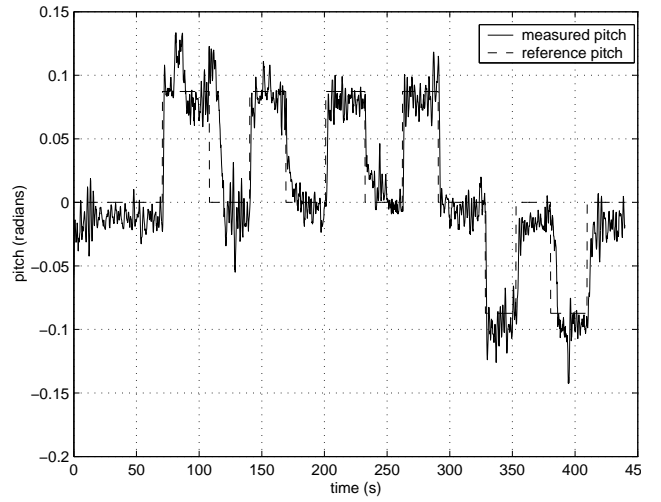


Figure 10: Closed loop pitch command response: $V=0.743$ m/sec. $k_p=11$

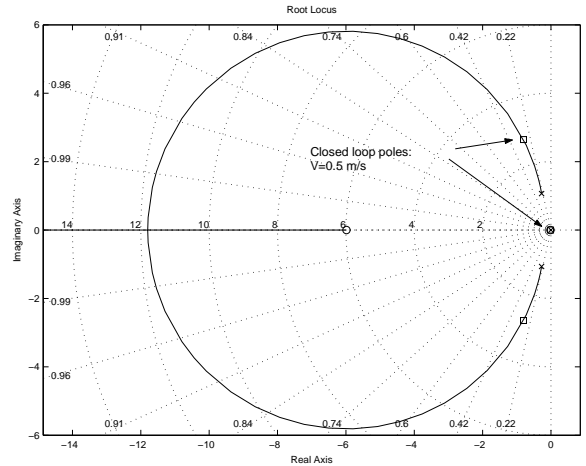


Figure 11: Pitch loop root locus as waterspeed varies: $k_p=12$, $k_d=2$, $k_i=0.2$, Design point $V=0.5$ m/sec.

Depth control

The pitch control loop is nested inside a depth loop, using a pressure transducer as the feedback element. A proportional plus differential controller is used to stabilise the loop. In order to get the depth transfer function we linearise the depth equation:

$$\dot{z} = -\sin \theta u + \cos \theta \sin \phi v + \cos \theta \cos \phi w \quad (8)$$

Assuming small vehicle perturbations about $\theta = 0$, $\phi = 0$, $u=V$, $v=0$, $w=0$ and dropping any term higher than first order, we get the following linear equation.

$$\dot{z} = -V\theta \quad (9)$$

Taking the Laplace transform, we arrive at the desired open loop transfer

$$G_z(s) = \frac{z(s)}{\theta(s)} = -\frac{V}{s} \quad (10)$$

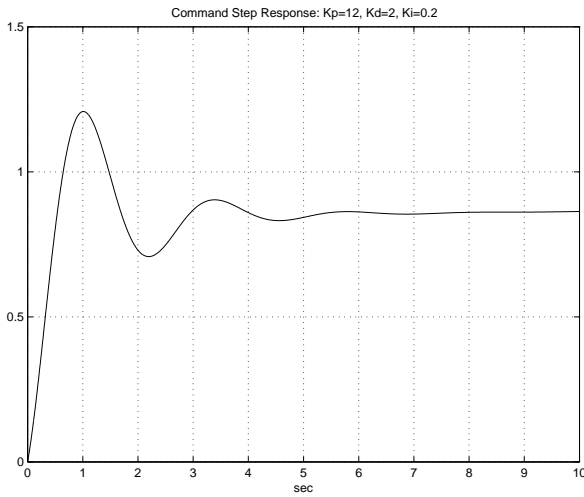


Figure 12: Command pitch step response: $k_p=12$, $k_d=2$, $k_i=0.2$, Design point $V=0.5$ m/sec.

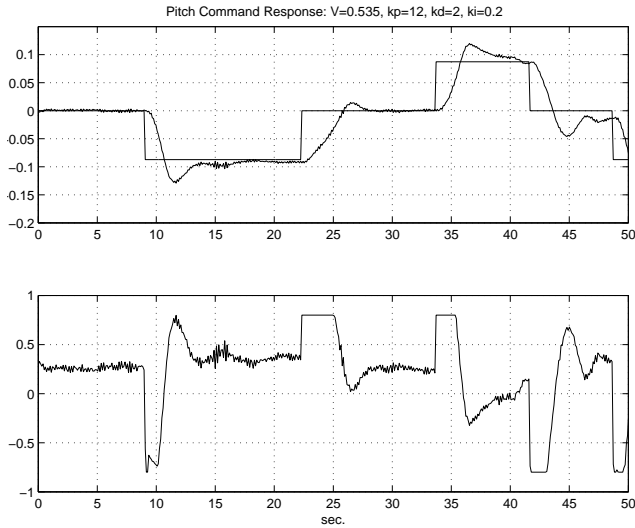


Figure 13: Closed loop pitch command response: $V=0.535$ m/sec. $k_p=12$, $k_d=2$, $k_i=0.2$

Figure 15 shows the simulated response to a depth command step input. In this simulation, saturation limits were placed on both the stern plane angle demand (0.23 rad.) and the pitch command (0.46 rad.).

Heading control

Heading control is achieved using a magnetometer to provide directional feedback. Symmetry of the submarine dictates that the pitch and yaw force/moment coefficients are identical. The only difference which arises in the transfer functions (Equations 1 and 2) is through the effects, in the pitch transfer function, caused by the relative positioning between the centres of buoyancy and gravity. This has very little effect on tuning the controller. A PID control loop, with similar gains to the pitch control loop may be applied to

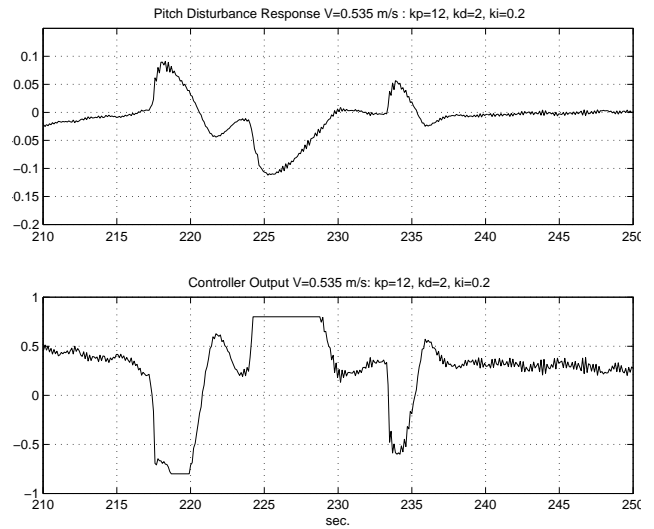


Figure 14: Closed loop pitch disturbance response: $V=0.535$ m/sec. $k_p=12$, $k_d=2$, $k_i=0.2$

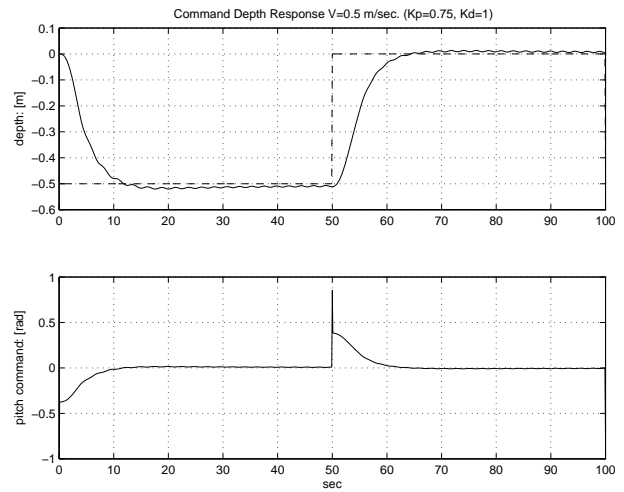


Figure 15: Command depth step response: $k_p=0.75$, $k_d=1$, $k_i=0$, Design point $V=0.5$ m/sec.

provide a stable yaw (heading angle) response.

Roll control

The roll dynamics, as predicted by Equation 6, are independent of the water speed. Figure 16 shows the simulated roll response to a command step input.

Conclusions

This paper has developed control loops which individually stabilise yaw, pitch and roll axes of the submarine. It is clear, however, from the original model that the dynamics between these axes is coupled. We predict that separate control of each axis will be adequate for small perturbations about straight and level cruising conditions. It remains to be seen whether coordinated turns, where rotations about all three axes occur simultaneously, are achievable.

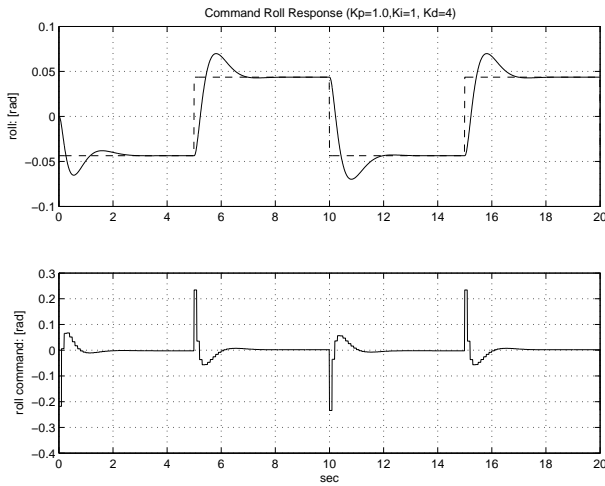


Figure 16: Command roll step response: $k_p=1.0$, $k_d=4.0$, $k_i=1.0$.

Acknowledgements

The authors wish to acknowledge the support of Queensland University of Technology, Schools of Mechanical and Civil Engineering who manufactured the submarine and provided the experimental test facilities. Design of the submarine and experimental facilities and laboratory measurements were by QUT undergraduate students Sam Reid and Simon Chambers. The staff of the CSIRO, Automation Group of Automation Group at CMST, designed and manufactured the submarine computing and control electronics and software and also undertook field trials of the submarine. CSIRO sponsored Julien Fontan, during 2002, as a visiting scholar from Ecole Centrale de Nantes (France).

References

Ridley P., Fontan J., Corke P. [2003], Submarine dynamic modeling, Proceedings Australian Conference on Robotics and Automation, 2nd - 4th December, 2003, Brisbane pp? - ?

Appendix

Modeling Parameters

| Symbol | Magnitude | Units |
|------------------|-----------|--------------------------|
| m | 18.826 | kg |
| W | 184.7 | N |
| I_{xx} | 1.77 | kg.m^2 |
| I_{yy} | 1.77 | kg.m^2 |
| I_{zz} | 0.0727 | kgm^2 |
| X_g | 0.003 | m |
| Z_g | 0.0048 | m |
| $N_{uu\delta_r}$ | -6.08 | kg.rad.^{-1} |
| $M_{uu\delta_r}$ | -6.08 | kg.rad.^{-1} |
| $K_{uu\delta_r}$ | 4.48 | kg.rad.^{-1} |
| $N_{\dot{r}}$ | -4.34 | kg.rad^{-2} |
| $M_{\dot{r}}$ | -4.34 | kg.rad^{-2} |
| $K_{\dot{r}}$ | -0.041 | kg.rad^{-2} |
| N_{uv} | 24 | kg |
| M_{uv} | -24 | kg |
| M_{uq} | -4.93 | kg.m.rad^{-1} . |
| N_{ur} | -4.93 | kg.m.rad^{-1} . |